

# Circular Polarization Diversity in Indoor Wireless Mobile Environments

Deock-Ho Ha · Yeon-Hwa Ko · Jae-Sung An · Tai-Hong Kim

## Abstract

In this paper, with the aim of achieving the expected performance improvement for a polarization diversity system, we analyzed two-branch polarization diversity at the receiving end of a mobile link which a transmitter emits circularly polarized wave. In this analysis, to calculate the correlation coefficient considered by XPD(cross polarization discrimination) between the two received signals, a simple theoretical model of circular polarization diversity is adopted. From the analysis results, it is clearly seen that the correlation coefficient of circular polarization diversity evaluated by the XPD is less than that of conventional linear polarization diversity. And also, we designed and implemented a circular polarization diversity system with micro-strip antenna. By using the circular polarization diversity system, we analyzed the measured data in indoor NLOS(Non-Line-Of-Sight) environments. From this analysis results, it is also clearly seen that the diversity effect of circular polarization diversity system shows better performance compared to the conventional linear diversity system by about 3 dB high.

**Key words** : Circular Polarization Diversity, Cross Polarization Discrimination(XPD), Micro-Strip Antenna.

## I. Introduction

Diversity schemes are the most useful in reducing multipath fading signals in mobile radio channels as it is well known. At present, both space diversity and polarization diversity have been mainly utilized in the base station diversity reception system<sup>[1]~[6]</sup>. And, in order to estimate diversity effect, the correlation coefficient between the signal envelopes has been widely used. In general, it is well known that effective diversity can be achieved by a correlation coefficient as long as the value is less than approximately 0.7<sup>[7],[8]</sup>. To keep the value below 0.7, space diversity requires antenna separation up to the 20 wavelengths. It is sometimes difficult to mount the diversity antenna on a tower with two antennas spaced by 20 wavelengths.

On the other hand, polarization diversity at the base station does not require antenna space because of the co-planer antenna configuration. If a micro-strip antenna implemented by two co-planer polarization antennas is used, the polarization diversity system can be easily implemented without space intervals. In [9], [10], an expression of correlation coefficient is derived from signal envelopes received by each polarization diversity branch at the station where the elevation angle of the ray is zero(2-D). In [11], an expression for the correlation coefficient and average branch signal levels is

also derived for the case of oblique incidence where the elevation angle is not zero(3-D). In this case, two-branch polarization diversity at the receiving end of a mobile link is analyzed when the transmitter emits a linearly polarized signal.

In this paper, we discuss a circular polarization diversity reception scheme in which circularly polarized signals radiated from the transmitting end are received by  $a \pm a$  polarized base station antenna. An expression of correlation coefficient considered XPD factor for a circular polarization diversity model is derived from oblique incidence which the elevation angle is not occurs. And we also designed and implemented a circular polarization diversity system using circularly polarized antenna at the transmitting unit. To estimate performance of the circular polarization diversity system, propagation characteristic measurements were carried out in an indoor NLOS radio environment.

## II. Theoretical Model of Circular Polarization Diversity

Polarization diversity at the base station does not require antenna spacing because of a co-planer antenna implemented by micro-strip substrate can be used. If a micro-strip antenna implemented by two co-planer polarization antennas is used as shown in Fig. 1, the polarization diversity system can be easily fabricated<sup>[12]</sup>.

Manuscript received June 8, 2004 ; revised September 9, 2004. (ID No. 20040608-020J)  
Dept. of Telecommunication Eng., Pukyong National University.

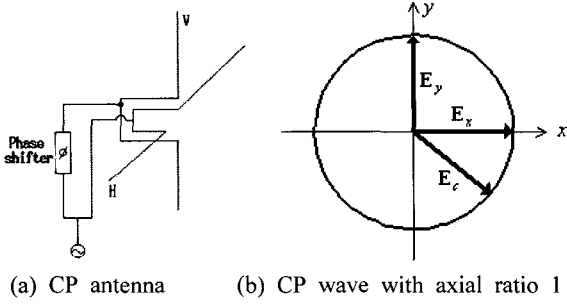


Fig. 1. Principle of circular polarization antenna configuration.

Fig. 1 shows the configuration of a circular polarization antenna. We fabricated a circular polarization antenna composed by two co-planer micro-strip antennas (a vertical and a horizontal micro-strip antenna with 90 degree phase shifter).

Generally, the circular polarized waves are expressed as follows;

$$E_{RC} = E_H + jE_V, \quad (1a)$$

$$E_{LC} = E_H - jE_V, \quad (1b)$$

where,  $E_{RC}$  is the electric field of right-handed circular polarization and  $E_{LC}$  is the electric field of left-handed circular polarization. Also, the signal arriving at the receiving end consists of vertical and horizontal polarized components and the two polarized components are expressed as follows;

$$E_H = e \cos(\omega t + \phi), \quad (2a)$$

$$E_V = e \cos(\omega t + \phi), \quad (2b)$$

where, it is assumed that  $e$  has independent Rayleigh distribution<sup>[13]</sup>,  $\phi$  has independent and uniformly distributed.

The vector form of equation (1) can be represented as follows;

$$\begin{aligned} \vec{E}_{RC} = & e_R \cos(\omega t + \phi_R) \vec{u}_1 \\ & + e_R \cos(\omega t + \phi_R + \frac{\pi}{2}) \vec{u}_2, \end{aligned} \quad (3a)$$

$$\begin{aligned} \vec{E}_{RL} = & e_L \cos(\omega t + \phi_L) \vec{u}_1 \\ & + e_L \cos(\omega t + \phi_L - \frac{\pi}{2}) \vec{u}_2, \end{aligned} \quad (3b)$$

where,

$$\vec{u}_1 = -\sin \phi \vec{x} + \cos \phi \vec{y}, \quad (4a)$$

$$\begin{aligned} \vec{u}_2 = & -\sin \nu \cos \phi \vec{x} - \sin \nu \sin \phi \vec{y} \\ & + \cos \nu \vec{z}. \end{aligned} \quad (4b)$$

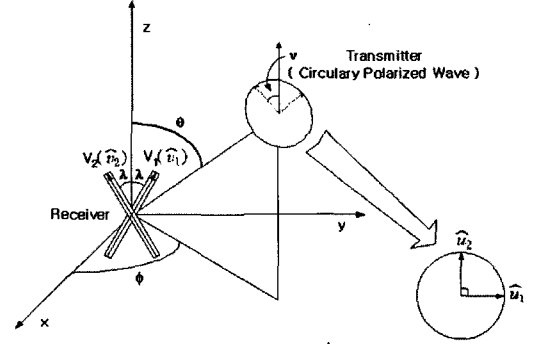


Fig. 2. Reception model of circular polarization diversity.

The unit vector  $\vec{u}_1$  and  $\vec{u}_2$  are perpendicular to the direction of propagation.

Fig. 2 is the model of circularly polarized diversity. As shown in Fig. 2, a transmitting antenna emits circularly polarized signal while the receiving end uses a two-branch polarized diversity antenna. Let the receiving antenna system be positioned at the origin, and the angular location of the transmitter is given by  $\phi$  and  $\theta$  from the origin, both of which are oriented at an angle  $\nu$  from the positive  $z$ -axis. It is also assumed that the transmitter and receiver ends are located in an urban environment and they are sufficiently far away to produce a Rayleigh distributed signal at the receiver.

In Fig. 2, when the expression of each unit vector of two-branch received diversity branches is the same as equation (5), the received electric field to each branch is represented as equation (6).

$$\vec{v}_1 = \sin \lambda \vec{y} + \cos \lambda \vec{z} \quad (5a)$$

$$\vec{v}_2 = -\sin \lambda \vec{y} + \cos \lambda \vec{z} \quad (5b)$$

$$V_1 = E_{RC} \cdot \vec{v}_1 + E_{LC} \cdot \vec{v}_1 \quad (6a)$$

$$V_2 = E_{RC} \cdot \vec{v}_2 + E_{LC} \cdot \vec{v}_2, \quad (6b)$$

where, the electric field of one branch is the same as equation (7).

$$\begin{aligned} V_1 = & \{e_R \cos(\omega t + \phi_R)(\cos \phi \sin \lambda) \\ & + e_R \sin(\omega t + \phi_R)(-\sin \nu \sin \phi \sin \lambda) \\ & + e_R \sin(\omega t + \phi_R)(\cos \nu \cos \lambda)\} \\ & + \{e_L \cos(\omega t + \phi_L)(\cos \phi \sin \lambda) \\ & + e_L \sin(\omega t + \phi_L)(\sin \nu \sin \phi \sin \lambda) \\ & - e_L \sin(\omega t + \phi_L)(\cos \nu \cos \lambda)\} \end{aligned} \quad (7)$$

Also, if  $a = \sin \lambda \cos \phi$

$$b = \cos \nu \cos \lambda - \sin \nu \sin \phi \sin \lambda,$$

Equation (7) can be expressed as equation (8).

$$\begin{aligned}
 V_1 = & \{e_R(a \cos \phi_R + b \sin \phi_R) \\
 & + e_L(a \cos \phi_L - b \sin \phi_L)\} \cos wt \\
 & - \{e_R(a \sin \phi_R - b \cos \phi_R) \\
 & + e_L(a \sin \phi_L + b \cos \phi_L)\} \sin wt
 \end{aligned} \quad (8)$$

From the above equations, received signal magnitude of the  $V_1$  branch is expressed as equation (9).

$$\begin{aligned}
 A_1 = & \{(e_R(a \cos \phi_R + b \sin \phi_R) \\
 & + e_L(a \cos \phi_L - b \sin \phi_L))^2 \\
 & + (e_R(a \sin \phi_R - b \cos \phi_R) + \\
 & e_L(a \sin \phi_L + b \cos \phi_L))^2\}^{1/2} \\
 = & \{(a^2 + b^2)(e_R^2 + e_L^2) + \\
 & 2e_R e_L((a^2 - b^2) \cos(\phi_R - \phi_L) \\
 & + 2ab \sin(\phi_R - \phi_L))\}^{1/2}
 \end{aligned} \quad (9)$$

Received signal magnitude of  $V_2$  can be also derived in the same way as  $V_1$ .

$$\begin{aligned}
 V_2 = & \{-e_R \cos(wt + \phi_R)(\cos \phi \sin \lambda) \\
 & + e_R \sin(wt + \phi_R)(\sin \nu \sin \phi \sin \lambda) \\
 & + e_R \sin(wt + \phi_R)(\cos \nu \cos \lambda)\} \\
 & + \{-e_L \cos(wt + \phi_L)(\cos \phi \sin \lambda) \\
 & - e_L \sin(wt + \phi_L)(\sin \nu \sin \phi \sin \lambda) \\
 & - e_L \sin(wt + \phi_L)(\cos \nu \cos \lambda)\}
 \end{aligned} \quad (10)$$

Substituting both equation  $a = \sin \lambda \cos \phi$  and  $c = \cos \nu \cos \lambda + \sin \nu \sin \phi \sin \lambda$  into the above equation, formula (10) can be re-expressed as follows;

$$\begin{aligned}
 A_2 = & \{(a^2 + c^2)(e_R^2 + e_L^2) + \\
 & + 2e_R e_L((a^2 - c^2) \cos(\phi_R - \phi_L) \\
 & - 2ab \sin(\phi_R - \phi_L))\}^{1/2}
 \end{aligned} \quad (11)$$

In general, the formula of correlation coefficient( $\rho$ ) and XPD are represented as follows;

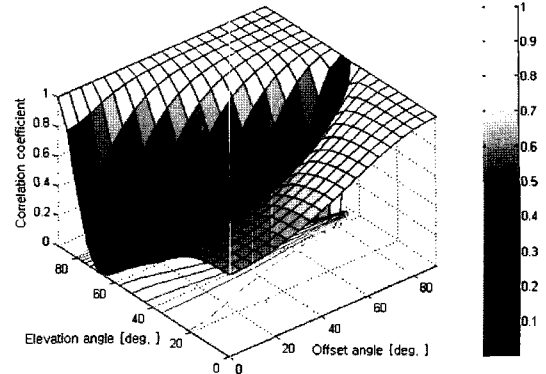
$$\rho = \frac{\langle A_1^2 \cdot A_2^2 \rangle - \langle A_1^2 \rangle \langle A_2^2 \rangle}{[(\langle A_1^4 \rangle - \langle A_1^2 \rangle^2)(\langle A_2^4 \rangle - \langle A_2^2 \rangle^2)]^{1/2}} \quad (12)$$

$$XPD = \frac{\langle e_R^2 \rangle}{\langle e_L^2 \rangle} \equiv \Gamma \quad (13)$$

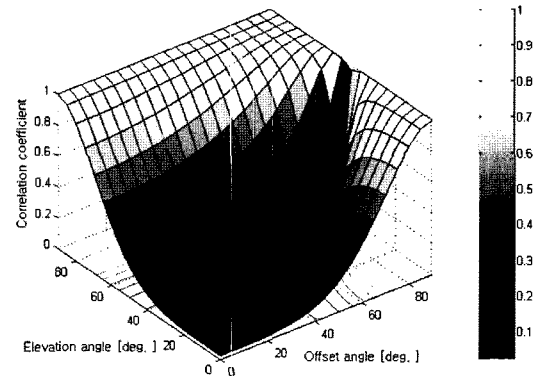
Therefore, by substituting equation (9), (11), (13) into equation (12), correlation coefficient considered XPD factor is given by equation (14).

$$\rho = \frac{(a^2 + b^2)(a^2 + c^2)(1 + \Gamma^2) + 2\Gamma(a^2 - b^2)(a^2 - c^2) - 8\Gamma a^2 b c}{[(a^2 + b^2)^2(a^2 + c^2)^2(1 + \Gamma^2)^4]^{1/2}} \quad (14)$$

From the empirical measurement data, Cross Pola-



(a) The conventional liner polarization diversity (XPD: 8.3 dB,  $\lambda = 45^\circ$ )



(b) The circular polarization diversity (XPD: 1.4 dB,  $\lambda = 45^\circ$ )

Fig. 3. Correlation coefficient for the two models.

zation Discrimination(XPD) value using circularly polarized diversity system indicate lower value about 6~7 dB than that of the case of using linear polarization at the transmitting end [12]. From this reason, to investigate the effect of XPD factor we plot the correlation coefficient difference between circular polarization and linear polarization diversity. Fig. 3 shows a correlation coefficient in 3D diagram when linearly polarized antenna and circularly polarized antenna are used at the transmitting end, respectively. As shown in Fig. 3, correlation coefficient value of circular polarization diversity is much lower than that of conventional linear polarization diversity because in the case where the circular polarized wave is applied, therefore XPD value is also much lower than that of the linear polarized wave. So it can be predicted that circular polarization diversity is a very effective diversity technique to reduce the multipath fading in indoor wireless environments.

### III. Circular Polarization Diversity System

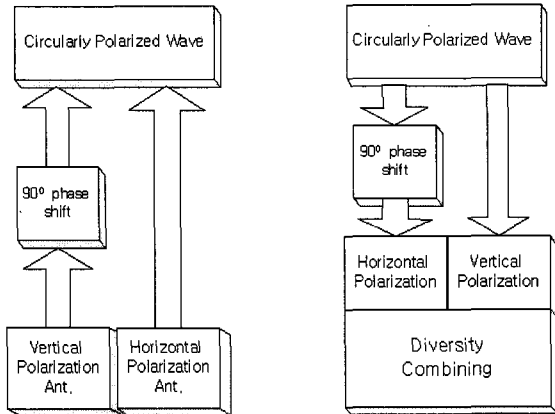


Fig. 4. Circuit configuration diagram of circular polarization diversity system.

3-1 Circularly Polarized Antenna(Transmitting Unit)

In order to certify the better performance of circular polarization diversity we implemented the diversity circuits and micro-strip antenna for measuring the signal strength in indoor wireless environments.

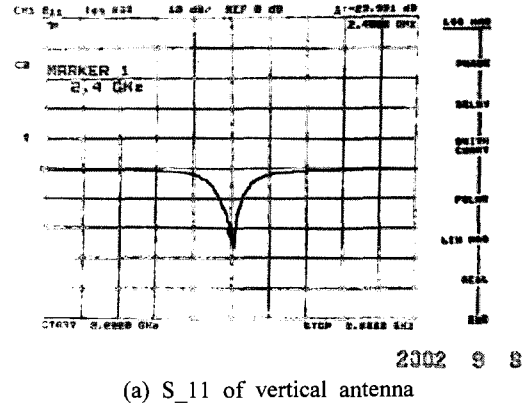
Fig. 4 is the diagram of circular polarization diversity system, which divides Transmitter and Receiver units.

Fig. 5 is a picture of the implemented transmitting unit. It is composed of vertical and horizontal polarization antennas and 90° Hybrid combiner using micro-strip substrate.

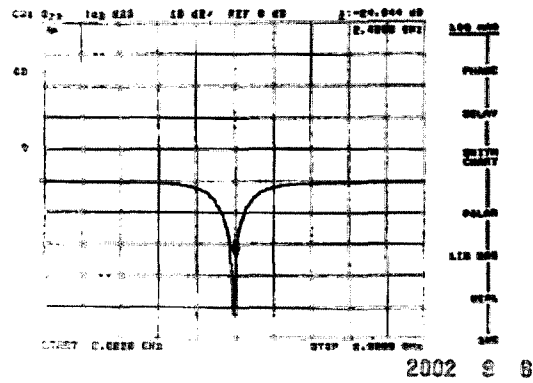
Fig. 6 shows return loss ( $S_{11}$ ) of the vertical and horizontal polarization antennas. The  $S_{11}$  of the vertical and horizontal polarization antennas is about -23 dB at center frequency 2.4 GHz. Fig. 7 and Fig. 8 show power divider factor and phase of the implemented 90° hybrid combiner. From the Fig. 7 and 8, we can see that the implemented combiner showed an insertion loss of 3 dB and the phase difference was well measured at precise 90° phase.



Fig. 5. Picture of the implemented transmitting antenna unit.



(a)  $S_{11}$  of vertical antenna



(b)  $S_{11}$  of horizontal antenna

Fig. 6. Comparison of the measured  $S_{11}$ .

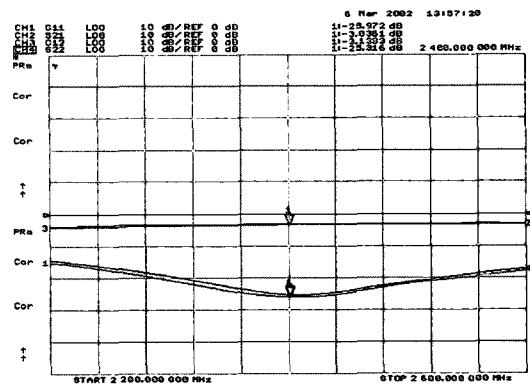
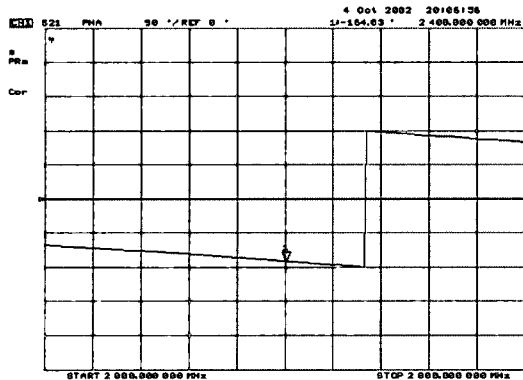
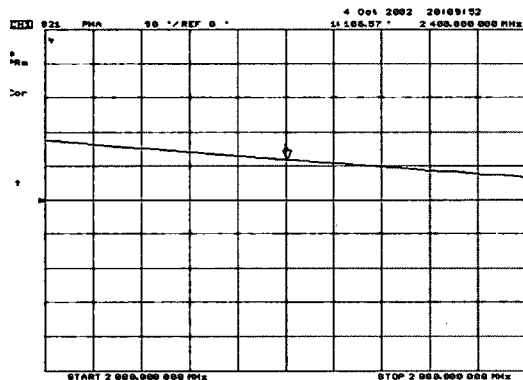


Fig. 7. Divider factor( $S_{12}$ ) of fabricated 90° phase Hybrid combiner.

Fig. 9 shows the radiation pattern of circular polarized antenna. For Axial ratio of circular polarization antenna, we measured radiation pattern at 0°, 45°, 90° and 135° of the standard antenna. It can be seen that ratio of the circular polarization antenna is about 0 dB, the gain of the fabricated circular polarization antenna is 2.7 dBi, and gain of the fabricated vertical and



(a) Phase of  $S_{12}(-164^\circ)$



(b) Phase of  $S_{13}(106^\circ)$

Fig. 8. Phase result of the fabricated  $90^\circ$  hybrid combiner.

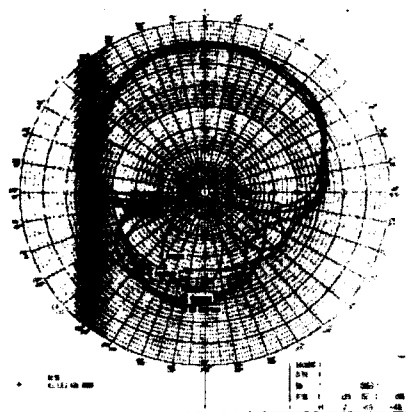


Fig. 9. Radiation pattern for the implemented CP Antenna.

horizontal polarization antenna is 5.7 dBi.

### 3-2 Polarization Diversity Combiner(Receiving Unit)

Fig. 10 shows a schematic diagram of the proposed polarization diversity combiner. It is composed of

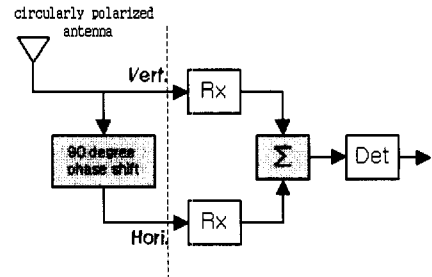


Fig. 10. Schematic diagram of the circular polarization diversity reception unit.

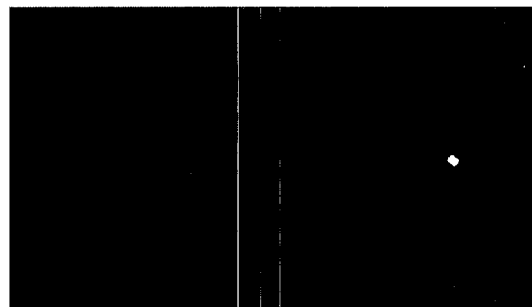
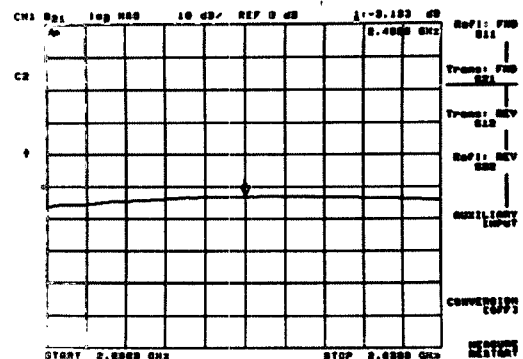
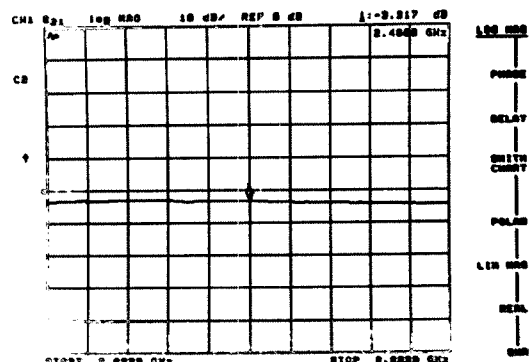


Fig. 11. Picture of the implemented diversity reception unit.

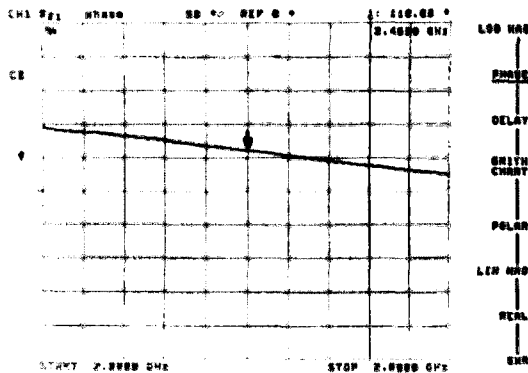


(a)  $S_{12}$  of the power divider

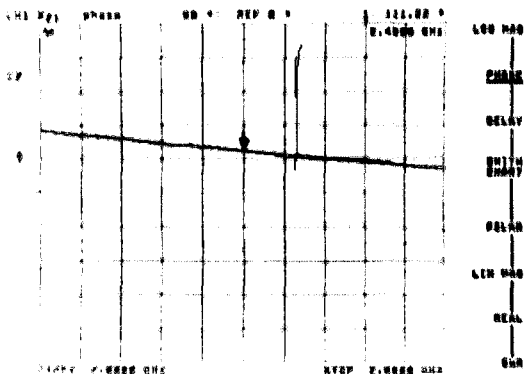


(b)  $S_{13}$  of the power divider

Fig. 12. Characteristics of diversity combiner.



(a) Phase of S<sub>12</sub>



(b) Phase of S<sub>13</sub>

Fig. 13. Phase difference of polarization diversity combiner.

vertical and horizontal antennas and 90° Hybrid combiner using micro-strip substrate. Fig. 11 shows a picture of the implemented polarization diversity reception unit.

Fig. 12 and Fig. 13 show the gains and the phase of the implemented polarization diversity combiner, respectively. In the Fig. 12 and Fig. 13, it can be seen that divider power S<sub>12</sub> and S<sub>13</sub> have insertion loss of 3 dB and 0° phase difference.

#### IV. The Measurement Results of Indoor Radio Environment

##### 4-1 The Measurement Environment(A)

To estimate the performance of fabricated circular polarization diversity system, we have conducted moving measurements in an indoor radio environment. Fig. 14 shows the measurement environment(A), where the office size is 11.11 m × 7.99 m × 2.7 m. The transmitting unit is propagated at a center frequency of 2.4

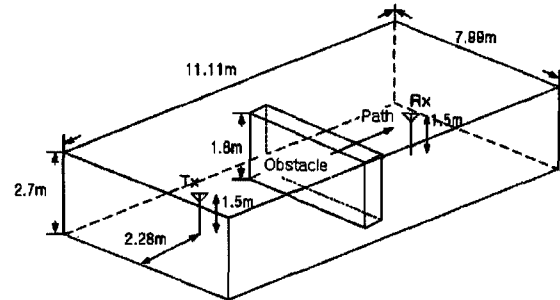


Fig. 14. Indoor radio measurement environment(A).

GHz using the signal generator. The received signal strength and distance pulse data are recorded automatically by a DAT(SONY 204A).

First, to estimate the implemented circular polarization antennas, we measured the signal strength using the following several antenna combinations: a) Right-handed Circular polarization at transmitting and receiving units(C-C), b) Right-handed Circular polarization at transmitting unit and Left-handed Circular polarization at receiving unit(C-X), c) Vertical polarization at transmitting and receiving units(V-V), d) Horizontal polarization at transmitting and receiving units(H-H) in indoor Line-Of-Sight(LOS) environment.

As shown in Fig. 15, average signal strength of the C-C case is better by 15 dB than that of C-X case.

Fig. 16 shows measured signal strength characteristic using fabricated circular polarization diversity system and conventional polarization diversity system in indoor NLOS environment. Fig. 17 shows accumulation probability distribution for the data of Fig. 16. From the Fig. 17, it can be seen that the proposed diversity effect of circular polarization diversity system has 3 dB better than conventional polarization diversity system in 1% accumulation probability.

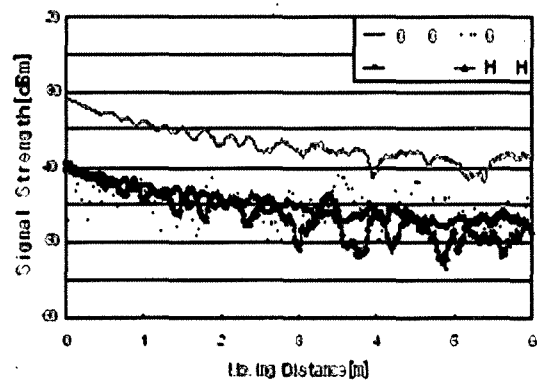


Fig. 15. Signal strength for moving measurement in LOS.

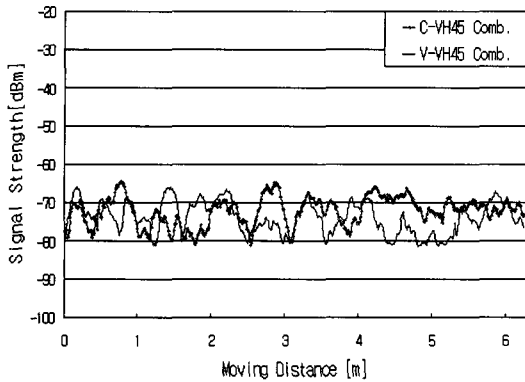


Fig. 16. Signal strength for moving measurement in NLOS.

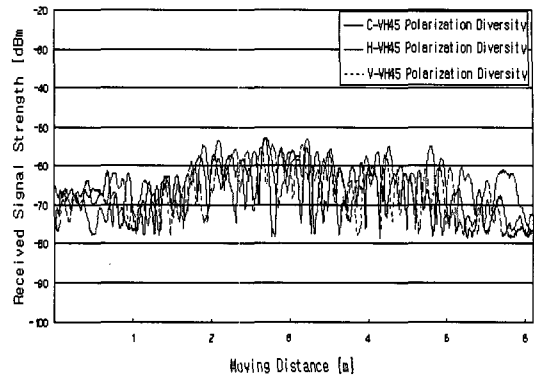


Fig. 19. Signal strength for moving measurement in NLOS.

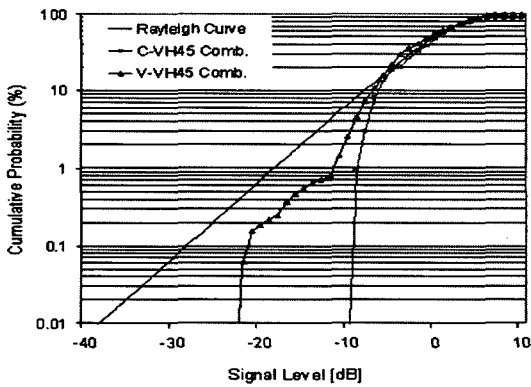


Fig. 17. Performance estimation for accumulation probability distribution.

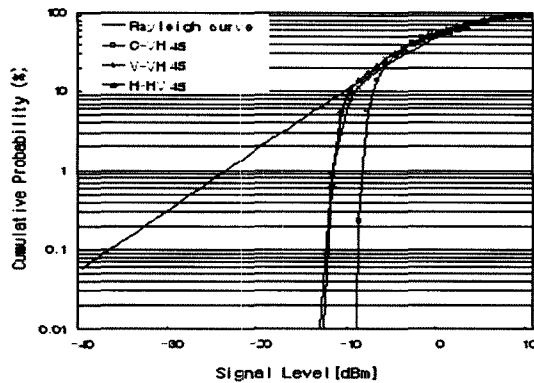


Fig. 20. Performance estimation for cumulative probability distribution.

#### 4-2 Indoor Radio Wave Measurement Environment(B)

The second measurement environment is a corridor with concrete wall in NLOS environment. In the Fig.

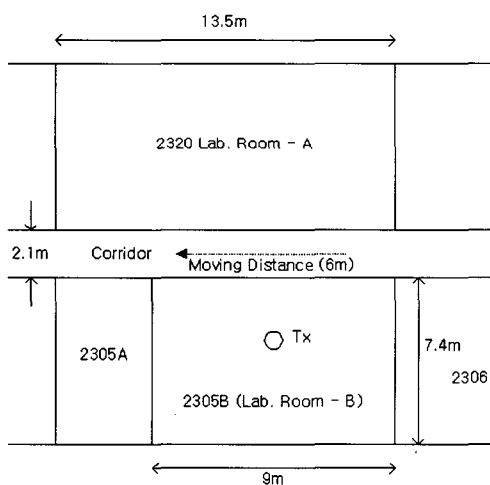


Fig. 18. Measurement environment(B).

18, transmitting antenna is mounted in Room(B), and signal strength is measured through aisle. Transmission and receiver antenna height are set at 1.4 m and the moving measurement distance is set at 6 m.

Fig. 19 shows measured signal strength characteristic for C-VH45, V-VH45 and H-VH45 in indoor NLOS environment. In this case, the character 45 indicates the linearly polarized signal with 45° degree, for the V (Vertically polarized wave) and H(Horizontally polarized wave) branches, respectively. Fig. 20 shows accumulation probability distribution for the Fig. 19. From the Fig. 20, it confirms that the circular polarization diversity system has about 3 dB gain in comparison with the conventional polarization diversity over cumulative probability density function 1 %.

#### V. Conclusions

In this paper, with the aim of reducing the multipath fading in indoor wireless environments, we proposed a

polarization diversity system using circular polarization antenna at transmitting end. From the analysis of proposed circular polarization diversity system, it was found that correlation coefficient value of the proposed circular polarization diversity system show lower value than that of conventional linear polarization diversity. To estimate proposed system performance, we have also measured propagation characteristic with a vehicle in motion using the implemented circular and conventional polarization diversity systems in indoor NLOS environments. From these measurements, it was also found that the diversity effect of the proposed circular polarization diversity scheme was improved by about 3 dB compared to the conventional polarization diversity reception method using linearly polarized antenna combination.

This work was done as a part of University Research Program supported by Ministry of Information & Communication in republic of Korea and supported by the Brain Busan 21 Project in 2004.

University Research Program supported by Ministry of Information & Communication in republic of Korea and supported by the Brain Busan 21 Project in 2004.

### References

- [1] W. C. Y. Lee, "Antenna spacing requirement for a mobile radio base-station diversity", *The Bell System Technical Journal*, vol. 50, no. 8, pp. 1859-1876, Jul. 1971.
- [2] W. C. Y. Lee, "Effects on correlation between two mobile radio base-station antennas", *IEEE Transactions on Communications*, vol. Com-21, no. 11, Nov. 1973.
- [3] William C. Y. Lee, Y. S. YEH, "Polarization diversity system for mobile radio", *IEEE Transactions on Communications*, vol. Com-20, no. 5, Oct. 1972.
- [4] R. G Vaughan, "Polarization diversity in mobile communications", *IEEE Trans. Veh. Technology*, vol. 39, no. 3, pp. 177-186, 1990.
- [5] F. Lotse, J. -E. Berg, U. Forssen and P. Idahl, "Base station polarization diversity reception in macrocellular systems at 1,800 MHz", *Vehicular Technology Conference, 1996. IEEE 46th*, vol. 3, pp. 1643-1646, May 1996.
- [6] K. Fujimori, H. Arai, "Polarization characteristics under indoor micro/pico cell environments", *Tenth International Conference on Antennas and Propagation*, vol. 2, pp. 302-305, Apr. 1997.
- [7] D. G. Brennan, "Linear diversity combining techniques", *Proc. IRE*, pp. 1075-1102, Jun. 1959.
- [8] M. Sakamoto, S. Kozono and T. Hattori, "Basic study on portable radio telephone design", *Proc. 32nd IEEE Veh. Technol. Conference*, pp. 279-284, May 1982.
- [9] S. Kozono, H. Tsuruhara and M. Sakamoto, "Base station polarization diversity reception for mobile radio", *IEEE Trans. Veh. Technol.*, vol. VT-33, no. 4, pp. 301-306, Nov. 1984.
- [10] S. Sakagami, A. Akeyama, "Dependence of base station polarization diversity characteristics on polarization inclination angle at mobile station", *IEICE*, vol. J70-B, no. 3, pp. 385-395, Mar. 1987.
- [11] E. Shin, S. Safavi-Nacini, "A simple theoretical model for polarization diversity reception in wireless mobile environments", *IEEE International Symposium on Antennas and Propagation*, vol. 2, pp. 1332-1335, Aug. 1999.
- [12] Ju-Hyun Lee, "A study on the fabrication and performance estimation of a circularly polarized diversity system for multipath fading reduction in mobile wireless environments", *Ph.D. Dissertation, Pukyong National University, Busan, Korea*, Aug. 2003.
- [13] Y. Okumura, E. Ohmori and K. Fukuda, "Field strength and its variability in VHF and UHF land mobile service", *Rev. Elect. Commun. Lab.*, vol. 16, pp. 825-873, Sep.-Oct. 1968.



Deock-Ho Ha



He received the M.S. and Ph.D. degrees from Kyoto University in Kyoto, Japan in 1984 and 1987, respectively. He was a Research engineer with The Central Research Institute of LG Group in Seoul, Korea from 1979 to 1981, and with The Wireless Research Laboratory of Matsushita Electric Industrial Co. Ltd. in Osaka, Japan from March to August 1987. In 1987, he joined the faculty of Pukyong National University in Busan, Korea, where he is a Professor. His research interests include channel coding, modulation technique, diversity system, indoor/outdoor propagation modeling for the mobile communication and indoor wireless LAN.

Jae-Sung An



He received the B.E. degree from Busan University of Foreign Studies, and M.S. degree from Pukyong National University, Busan, Korea in 2002. He has been enrolled in a doctoral course in Pukyong National University, Busan, Korea since 2004. His research interests include MC-OFDM, multi-carrier system.

Yeon-Hwa Ko



She received the B.E. and M.E. degree from Dong-eui University, Pusan, Korea in 1996 and 1998, respectively. And she received Ph.D. degree from Pukyong National University, Busan, Korea in August 2004. Her research interests include turbo code, channel coding, space-time processing, multi-carrier system and propagation modeling for mobile communication.

Tai-Hong Kim



He received the B.E. degree from Dong-Seo University, Busan, Korea, in 2003. He is currently working toward the M.S degree in Pukyong National University. His current interests are antennas and mobile communication system.